

RSC Advances



This is an *Accepted Manuscript*, which has been through the Royal Society of Chemistry peer review process and has been accepted for publication.

Accepted Manuscripts are published online shortly after acceptance, before technical editing, formatting and proof reading. Using this free service, authors can make their results available to the community, in citable form, before we publish the edited article. This *Accepted Manuscript* will be replaced by the edited, formatted and paginated article as soon as this is available.

You can find more information about *Accepted Manuscripts* in the [Information for Authors](#).

Please note that technical editing may introduce minor changes to the text and/or graphics, which may alter content. The journal's standard [Terms & Conditions](#) and the [Ethical guidelines](#) still apply. In no event shall the Royal Society of Chemistry be held responsible for any errors or omissions in this *Accepted Manuscript* or any consequences arising from the use of any information it contains.

COMMUNICATION

Purification, organophilicity and transparent fluorescent bulks fabrication derived from hydrophilic carbon dots†

Cite this: DOI: 10.1039/x0xx00000x

Received 00th January 2014,
Accepted 00th January 2014

DOI: 10.1039/x0xx00000x

www.rsc.org/

Xiangyang Chen^{ab}, Zhijun Zhang^{c*}, Jingtai Zhao^{c*}

Oil/water interfacial self-assembly strategy was successfully used to purify hydrophilic carbon dots (CDs) synthesized by a typical hydrothermal method. Subsequently, organophilic octadecylamine (ODA)-capped carbon dots were obtained by further surface modification. Finally, transparent fluorescent bulks were fabricated through the above processes derived from hydrophilic carbon dots.

Carbon dots (CDs), as a novel kind of versatile fluorescence material, have drawn widespread attention owing to their high quantum yield, low cost, low toxicity and biocompatibility¹. The superior advantages of fluorescent CDs show promising applications in many fields, such as biomedical imaging², sensing^{3,4}, ion probe⁵, photocatalysts⁶ and solid-state optoelectronic devices⁷. Therefore, various approaches have been developed to synthesize CDs, such as laser ablation⁸, arc discharge⁹, electrochemical synthesis¹⁰, microwave methods¹¹, and hydrothermal method¹² where the CDs are broken off from a larger carbon source or form from molecular precursors (like citrate salts, glucose, PEG, and glycerol *et al.*¹³). Hydrothermal methods have been amazing investigated recently due to their simple preparation process, rich raw materials (inorganic salt¹⁴, fruits^{15,16}, protein^{17,18}, and organic waste¹⁹⁻²¹ *et al.*), and relatively high quantum yield (68% reported by Guo *et al.*²², 80% by Zhu *et al.*²³) compared with other methods²⁴. In summary, CDs prepared by hydrothermal methods have three features: (i) Quiet small size, mostly below 5nm; (ii) inevitable impurities, such as inorganic ions; (iii) water-soluble for rich hydrophilic groups are included on the surface, like hydroxyl and carboxyl. These CDs were usually conducted through dialysis tube for more than 24 h to remove impurities, and they were prone to use as aqueous solution due to their hydrophilicity. As a consequence, much time and distilled water are consumed, simultaneously applications in solid state photoelectric fields are greatly limited. Aiming at future development, a couple of possible strategies based on hydrothermal methods could be adopted. On one hand, effective purification routes can be attempted: in this case, time- and water-saving scheme is

desirable. On the other hand, solification of hydrophilic CDs to enlarge applications more than aqueous solution should be pursued.

Herein, we report a novel method for enrichment and purification of the hydrophilic CDs, and fabrication of transparent fluorescent bulks retained the mostly native characteristic emission of CDs solution. Firstly, a modified hydrothermal method according to a typical literature²² is used to synthesize CDs. High-resolution transmission electron microscopy (HRTEM), X-ray photoelectron spectroscopy (XPS), and photoluminescence spectroscopy are used to characterize the products. The diameter of the as-prepared CDs is about 3~5 nm (ESI† Fig. S1(a)), the lattice spacing of 0.308 nm and 0.258 nm is consistent with (002) and (020) diffraction planes of graphite^{25,26} (ESI† Fig. S1(b)). The survey of XPS indicates that carbon, nitrogen, oxygen and sodium element present in the surface of CDs (ESI† Fig. S1(c)), and C1s expanded peaks at 285.0, 286.5 and 288.3 can be assigned to carbon in the form of C-C, C-O and C=O/C=N, respectively^{3,14,27} (Fig. S1(d)). The blue-emitting under 365 nm UV light (Fig. S1(f)) and 6.38 ns of decay time (Fig. S1(e)) with characteristic excitation (355 nm) and emission wavelengths (435 nm) are consistent to the previous literatures^{28,29}. Secondly, Oil/water interfacial self-assembly strategy, which is widely used for various nanostructures into functional nanofilms³⁰⁻³⁶ from 0D nanoparticles to 2D nanoplatelets, have been attempted to enrich and purify the as-prepared CDs (experimental detail are shown in ESI†). The mechanism of oil/water interfacial self-assembly is reported as the reduction in the total interfacial energy of the system proved by Pieranski's thermodynamics model³⁷.

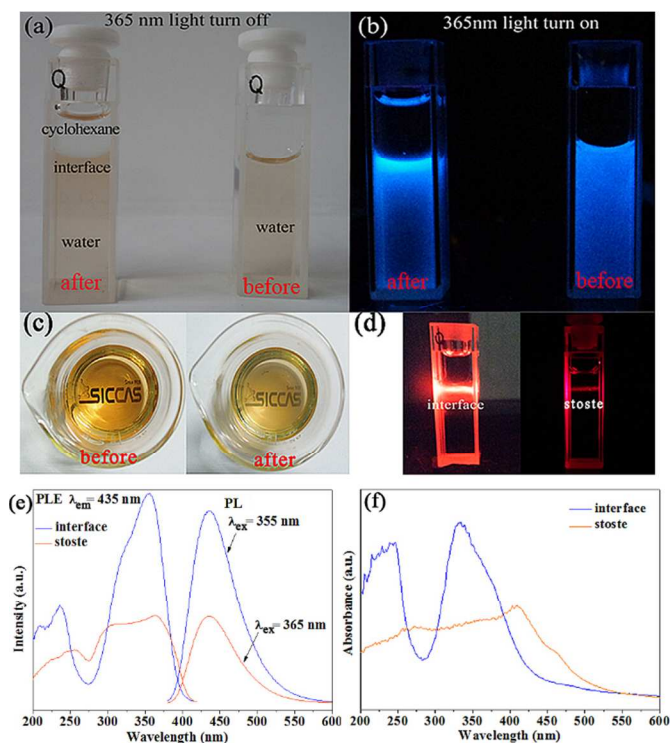


Fig. 1 (a)–(c) Comparison of CDs aqueous solution before and after oil/water self-assembly procedure, (d) tyndall effect of as-prepared CDs in the interface and stoste, (e) photoluminescence excitation and emission spectra of CDs in stoste and interface, (f) absorption spectra of CDs in stoste and interface.

The novel oil/water interfacial self-assembly strategy has been demonstrated to possess two mainly functions: enrichment and purification. Firstly, the explicit enrichment function for the as-prepared CDs is well presented in Fig. 1. It can be concluded that the CDs are enriched in cyclohexane/water interface because of the following three facts: (i) Interfacial emission intensity under 365 nm UV light is stronger than that of in water observed by naked eyes (Fig. 1(b)), which also can be demonstrated by photoluminescence and absorption spectra. As shown in Fig. 1(e) and (f), they clearly reveal that the photoluminescence and absorption intensity of interfacial CDs are 2~3 times stronger than those of stoste. One fact should be noted that the luminescence spectra of CDs stoste are wider and flatter, which might be ascribed to absorption of impurities. (ii) Significantly enhanced Tyndall effect in the interface compared with that of stoste because Tyndall effect is proportional to the concentration of the nanoparticles (about 1~100 nm) in some degree. (iii) The reduced transparency of the as-processed sample (Fig. 1(c)) also confirms the enrichment of CDs in the interface, due to the intensive absorption and scattering of light. It should be noted that oil/water self-assembly strategy is just a fast method to gather the CDs from stoste, which is a kind of “soft agglomeration”. This can be assigned to the following facts: On one hand, the reactant sodium citrate, as a kind of surfactant, can prevent the CDs to make a “hard linkage” by surrounding the CDs. On the other hand, the interfacial CDs were observed as been aggregated by TEM, however, the aggregated CDs can be diluted when dispersed in water again, as shown in Fig. 2S. As a result, the fluorescence of the CDs enhances obviously as the particles assemble at the oil/water interface, which is totally different with the previous report³⁸.

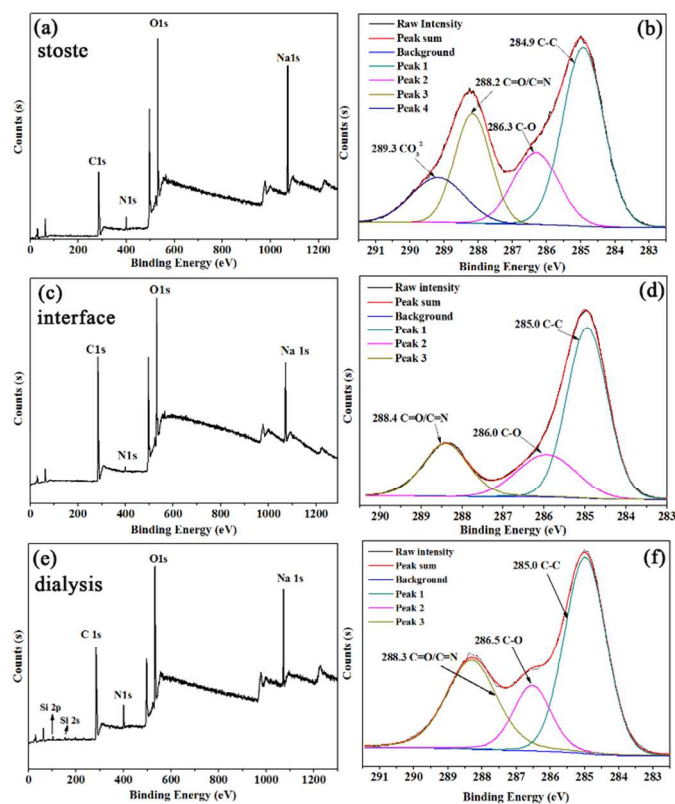


Fig. 2 XPS results of original CDs, and treated by oil/water self-assembly and dialysis (24 h), (a) (c) (e) total spectra of elements, (b) (d) (f) high-resolution spectra of C1s.

Secondly, the highly efficient purification of oil/water interfacial self-assembly for CDs can be clearly indicated by XPS results. Although there is no difference in the element types of all the samples (i.e. C, N, O and Na), the content of each element and bonding state of C element are different, as shown in Fig. 2 (detailed fitting results are tabled in Table S1 and S2 in ESI†). The content of Na, N element derived from reactant NH_4HCO_3 varies from 14.27 and 3.06 mol% to 5.94 and 1.82 mol% through oil/water interfacial self-assembly strategy, respectively. In addition, high-resolution spectrum of C1s shows that CDs stoste consisted of CO_3^{2-} group, which is no existing in the samples purified by oil/water interfacial self-assembly strategy. The fitting results indicate this novel strategy is an effective method to drive out the impurities (such as CO_3^{2-} , Na and N) from CDs stoste, which enhances the quantum yields (QYs) from about 29.1 % (stoste) to 36.5 % (interface). It should be noted that the increasing of C content and C-O/C-C bonds can be originated from ethanol ($\text{C}_2\text{H}_5\text{OH}$), which is used in oil/water interfacial self-assembly process.

In order to highlight the superiority of this novel method, some interesting comparisons have been carried out with the traditional dialysis with 24 h. There are three main remarkable advantages of oil/water interfacial self-assembly strategy: (i) From Table S1 in ESI†, it can be seen that the residual content of Na (impurity) through this novel method is 5.94 mol%, which is much less than dialysis for 24 h (7.02 mol%). (ii) The strategy is time- and water-saving, only about 10 minutes and little water are required over the whole process, while the traditional dialysis method is always carried out for 24 h and needs a mass of deionized water. (iii) The QYs of CDs purified by this novel method can reach as high as 36.5 %, which is higher than that of dialysis (34.7 %).

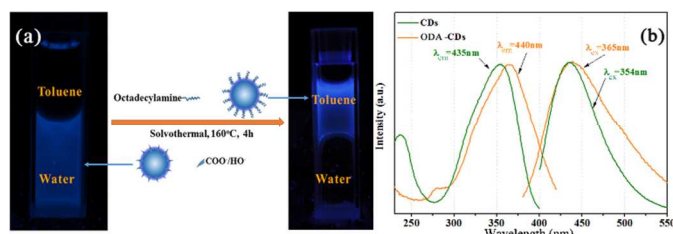


Fig. 3 (a) Schematic of CDs transfer from water to toluene, (b) excitation and emission spectra of CDs (in water) and ODA-CDs (in toluene). The spectra were normalized by divided maximum value of emission intensity.

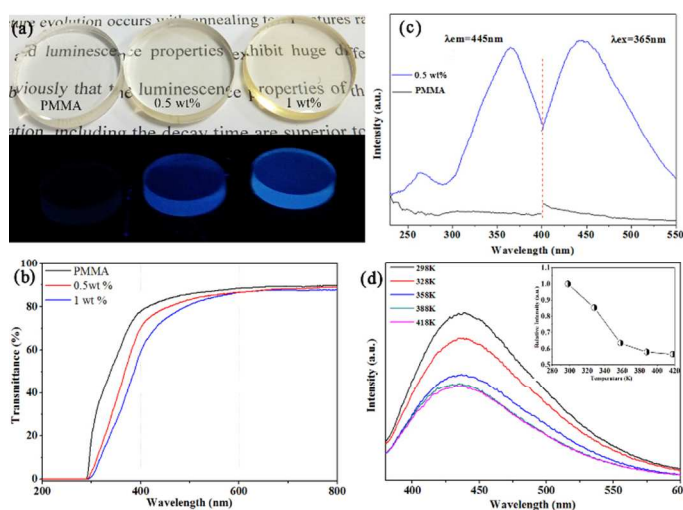


Fig. 4 (a) Digital photos of PMMA and ODA-CDs (0.5 and 1.0 wt%) embedded PMMA bulk (sample thickness 3.5 mm) under ambient and 365 nm UV light, (b) transmittance of as-fabricated samples, (c) typical excitation and emission spectra of ODA-CDs embedded sample (0.5 wt%), the pure PMMA bulk was measured under the same conditions as comparison, (d) variable temperature fluorescence spectra of the sample (0.5 wt%) (the inset shows the relative emission intensity with increasing temperature).

Composites that consist of polymer-inorganic hybrid material have been attractive owing to their enhanced mechanical, thermal, biological, magnetic, optical, electronic, and optoelectronic properties for solar cells, as compared to the corresponding inorganic or polymer component only³⁹⁻⁴¹. Polymethyl methacrylate (PMMA) as a common polymer, is always to be chosen as a matrix of inorganic owing to its excellent optical properties, such as PMMA-TiO₂⁴² and PMMA-ZnO⁴³. Therefore, fabrication of PMMA-based hybrid is a good method to realize the aiming at solification of CDs. Recently, Zhang *et al.*⁴⁴ and Liu *et al.*¹ have successfully embedded CDs into PMMA matrix, forming versatile multidimensional fluorescent materials. However, up to now, there is few report on homogenous dispersion of totally hydrophilic CDs in PMMA matrix, which is synthesized by hydrothermal method. Because two major obstacles must be overcome to obtain optically transparent PMMA-CDs hybrid material: (i) The immiscible polarity of hydrophobic and hydrophilic surfaces causes phases separation⁴¹; (ii) the CDs introduced are easy to reunite, causing light scattering and opaqueness. Here octadecylamine (ODA) as surface modifier is used to solve these two problems: On one hand, it is facile to convert the hydrophilic CDs into organophilicity because the -NH₂ group in ODA and -COOH group in CDs are easy to make covalent linking via the formation of amide linkages (-NHCO-) in a solvothermal reaction (more details in ESI†)⁴⁵. The Fourier transform infrared (FTIR) spectra of the ODA, CDs from stoste, and ODA-CDs purified from toluene indicate I and II bands of the amide linkage at

1644 and 1552 cm⁻¹, which is similar to the previous reports^{45, 46}, providing a direct proof of covalent attachment of ODA through the amide bond formation (Fig. S3 in the ESI†). On the other hand, ODA can bind to the surface of CDs, as a consequence, the CDs lose their conformational entropy and restrain agglomeration in the PMMA matrix by stereo-hindrance effect. Therefore, the as-modified organophilic ODA-CDs spontaneously transfer into toluene phase and show blue-emitting, while the lower aqueous phase loses much blue luminescence under 365 nm UV light irradiation (**Fig. 3(a)**). The photoluminescence properties of CDs and ODA-CDs are measured as shown in **Fig. 3(b)**. For their excitation spectra, the CDs reveal two sharp excitation bands with the peaks at 238 and 354 nm, whereas the ODA-CDs show only one distinct peak centred at 365 nm. Corresponding to the change of excitation spectra, the emission spectra also varies in shape and position. The emission band is observed to be red shifted from ~435 to ~440 nm and the full width at half maximum broadens from ~65 to ~100 nm, which might be assigned to the covalent linkage between “-NH-” and “-C=O”, leading to the decreasing of electron density of carboxyl.

Subsequently, ODA-CDs embedded PMMA transparent fluorescent bulks are fabricated as shown in **Fig. 4(a)**. The transmittance of the bulks have no obvious change in the range of 600-800 nm around 85% (**Fig. 4(b)**), while exhibit an optical-limiting effect over 300-600 nm, i.e. concentration-dependent red-shift, similar to their ZnO-PMMA counterparts⁴⁷. The bulk shows a typical blue emitting under 365 nm light excitation (**Fig. 4(c)**), which is similar to that of its ODA-CDs precursor (i.e. excitation peak at 365 nm, emission peak at 440 nm, **Fig. 3(b)**), indicating that the ODA-CDs particles have been well dispersed in PMMA and surface state has no remarkable change⁴⁴. As a comparison, the similar fluorescent bulks derived from the CDs purified by the dialysis method also have been fabricated, the transmittance of the as-prepared bulks are measured as shown in Fig. S4. It is clearly observed that there is no difference in the transmittance of “target bulks”, indicating this novel method may lead to more efficient way of application. In addition, the thermal quenching property of the hybrid material has been measured from 298 K (RT) to 418 K (**Fig. 4(c)**). There exists scarcely shift of all the emission peaks, and the emission intensity at 388 K can reach up to 60% of that at RT, revealing a good thermal quenching performance.

Conclusions

In summary, Oil/water interfacial self-assembly strategy has been successful carried out to enrich and purify hydrophilic CDs, which is more effective to enrich the products and remove impurities compared to the traditional dialysis method. In addition, bright blue-emitting ODA-CDs embedded PMMA bulk is successful fabricated derived from hydrophilic CDs, which is prepared by a typical hydrothermal method. The as-prepared fluorescent bulks show robust and stable luminescence property and good potential for solid state applications.

Acknowledgements

The authors gratefully acknowledge the support for this work from the National Natural Science Foundation of China under Grant No. 11104298 and U1332202. Innovation program of Shanghai Institute of Ceramics under Grant No. Y34ZC130G and the Open Fund of Key Laboratory of Transparent Opto-functional Inorganic Materials of Chinese Academy of Sciences. The authors also wish to acknowledge Professor Dr. Xinhua Zhong (ECUST, East China

University of Science and Technology) for his support with QYs calculation.

Notes and references

^a Key Laboratory of Transparent Opto-Functional Inorganic Materials of Chinese Academy of Sciences, Shanghai Institute of Ceramics, Shanghai 200050, PR China

^b University of Chinese Academy of Sciences, Beijing 100039, PR China

^c School of Materials Science and Engineering, Shanghai University, Shanghai 200072, PR China. E-mail: zhangzj@mail.sic.ac.cn (Z.J. Zhang), jtzhao@shu.edu.cn (J.T. Zhao)

[†] Electronic Supplementary Information (ESI) available: Experimental details, TEM images, XPS results, FTIR spectra, decay time measurement, digital photos of as-prepared CDs by hydrothermal method, detailed element contents and bonding variations of the CDs in different stages. See DOI: 10.1039/c002206c. See DOI:10.1039/c000000x/

- 1 S. S. Liu, C. F. Wang, C. X. Li, J. Wang, L. H. Mao and S. Chen, *J. Mater. Chem. C*, 2014, **2**, 6477-6483.
- 2 X. M. Yang, Y. Zhuo, S. S. Zhu, Y. W. Luo, Y. J. Feng and Y. Dou, *Biosens. Bioelectron.*, 2014, **60**, 292-298.
- 3 H. Nie, M. J. Li, Q. S. Li, S. J. Liang, Y. Y. Tan, L. Sheng, W. Shi and S. X. A. Zhang, *Chem. Mater.*, 2014, **26**, 3104-3112.
- 4 F. Lin, W. N. He and X. Q. Guo, *Adv. Mater. Res.*, 2012, **415-417**, 1319-1322.
- 5 X. Y. Teng, C. G. Ma, C. J. Ge, M. Q. Yan, J. X. Yang, Y. Zhang, P. C. Morais and H. Bi, *J. Mater. Chem. B*, 2014, **2**, 4631-4639.
- 6 H. Li, W. Q. Kong, J. Liu, M. M. Yang, H. Huang, Y. Liu and Z. H. Kang, *J. Mater. Chem. B*, 2014, **2**, 5652-5658.
- 7 C. X. Li, C. Yu, C. F. Wang and S. Chen, *J. Mater. Sci.*, 2013, **48**, 6307-6311.
- 8 Y. P. Sun, B. Zhou, Y. Lin, W. Wang, K. A. S. Fernando, P. Pathak, M. J. Meziani, B. A. Harruff, X. Wang, H. F. Wang, P. J. G. Luo, H. Yang, M. E. Kose, B. L. Chen, L. M. Veca and S. Y. Xie, *J. Am. Chem. Soc.*, 2006, **128**, 7756-7757.
- 9 X. Y. Xu, R. Ray, Y. L. Gu, H. J. Ploehn, L. Gearheart, K. Raker and W. A. Scrivens, *J. Am. Chem. Soc.*, 2004, **126**, 12736-12737.
- 10 J. G. Zhou, C. Booker, R. Y. Li, X. T. Zhou, T. K. Sham, X. L. Sun and Z. F. Ding, *J. Am. Chem. Soc.*, 2007, **129**, 744-745.
- 11 X. H. Wang, K. G. Qu, B. L. Xu, J. S. Ren and X. G. Qu, *J. Mater. Chem.*, 2011, **21**, 2445-2450.
- 12 B. F. Han, W. X. Wang, H. Y. Wu, F. Fang, N. Z. Wang, X. J. Zhang and S. K. Xu, *Colloid. Surface. B*, 2012, **100**, 209-214.
- 13 S. N. Baker and G. A. Baker, *Angew. Chem., Int. Ed.*, 2010, **49**, 6726-6744.
- 14 Z. Yang, M. H. Xu, Y. Liu, F. J. He, F. Gao, Y. J. Su, H. Wei and Y. F. Zhang, *Nanoscale*, 2014, **6**, 1890-1895.
- 15 S. Sahu, B. Behera, T. K. Maiti and S. Mohapatra, *Chem. Commun.*, 2012, **48**, 8835-8837.
- 16 B. De and N. Karak, *Rsc Adv.*, 2013, **3**, 8286-8290.
- 17 Z. Zhang, J. H. Hao, J. Zhang, B. L. Zhang and J. L. Tang, *Rsc Adv.*, 2012, **2**, 8599-8601.
- 18 C. Z. Zhu, J. F. Zhai and S. J. Dong, *Chem. Commun.*, 2012, **48**, 9367-9369.
- 19 J. M. Wei, J. M. Shen, X. Zhang, S. K. Guo, J. Q. Pan, X. G. Hou, H. B. Zhang, L. Wang and B. X. Feng, *Rsc Adv.*, 2013, **3**, 13119-13122.
- 20 J. J. Zhou, Z. H. Sheng, H. Y. Han, M. Q. Zou and C. X. Li, *Mater. Lett.*, 2012, **66**, 222-224.
- 21 J. M. Wei, X. Zhang, Y. Z. Sheng, J. M. Shen, P. Huang, S. K. Guo, J. Q. Pan, B. T. Liu and B. X. Feng, *New J. Chem.*, 2014, **38**, 906-909.
- 22 Y. M. Guo, Z. Wang, H. W. Shao and X. Y. Jiang, *Carbon*, 2013, **52**, 583-589.
- 23 S. J. Zhu, Q. N. Meng, L. Wang, J. H. Zhang, Y. B. Song, H. Jin, K. Zhang, H. C. Sun, H. Y. Wang and B. Yang, *Angew. Chem., Int. Ed.*, 2013, **52**, 3953-3957.
- 24 F. Y. Yan, Y. Zou, M. Wang, L. F. Dai, X. G. Zhou and L. Chen, *Prog. Chem.*, 2014, **26**, 61-74.
- 25 J. J. Niu, H. Gao, L. T. Wang, S. Y. Xin, G. Y. Zhang, Q. Wang, L. N. Guo, W. J. Liu, X. P. Gao and Y. H. Wang, *New J. Chem.*, 2014, **38**, 1522-1527.
- 26 X. Guo, C. F. Wang, Z. Y. Yu, L. Chen and S. Chen, *Chem. Commun.*, 2012, **48**, 2692-2694.
- 27 S. W. Yang, J. Sun, X. B. Li, W. Zhou, Z. Y. Wang, P. He, G. Q. Ding, X. M. Xie, Z. H. Kang and M. H. Jiang, *J. Mater. Chem. A*, 2014, **2**, 8660-8667.
- 28 A. Jaiswal, S. S. Ghosh and A. Chattopadhyay, *Chem. Commun.*, 2012, **48**, 407-409.
- 29 H. T. Li, H. Ming, Y. Liu, H. Yu, X. D. He, H. Huang, K. M. Pan, Z. H. Kang and S. T. Lee, *New J. Chem.*, 2011, **35**, 2666-2670.
- 30 Y. Ren, M. Chen, L. F. Hu, X. S. Fang and L. M. Wu, *J. Mater. Chem.*, 2012, **22**, 944-950.
- 31 L. F. Hu, L. M. Wu, M. Y. Liao and X. S. Fang, *Adv. Mater.*, 2011, **23**, 1988-1992.
- 32 Z. W. Niu, J. B. He, T. P. Russell and Q. A. Wang, *Angew. Chem., Int. Ed.*, 2010, **49**, 10052-10066.
- 33 J. Wang, D. Wang, N. S. Sobal, M. Giersig, M. Jiang and H. Moehwald, *Angew. Chem., Int. Ed.*, 2006, **45**, 7963-7966.
- 34 L. F. Hu, M. Chen, X. S. Fang and L. M. Wu, *Chem. Soc. Rev.*, 2012, **41**, 1350-1362.
- 35 Y. K. Park, S. H. Yoo and S. Park, *Langmuir*, 2007, **23**, 10505-10510.
- 36 Y. Lin, H. Skaff, T. Emrick, A. D. Dinsmore and T. P. Russell, *Science*, 2003, **299**, 226-229.
- 37 P. Pieranski, *Phys. Rev. Lett.*, 1980, **45**, 569-572.
- 38 P. F. Shen and Y. S. Xia, *Anal. Chem.*, 2014, **86**, 5323-5329.
- 39 Z. Ahmad, M. I. Sarwar and J. E. Mark, *J. Mater. Chem.*, 1997, **7**, 259-263.
- 40 I. M. Sero, J. Bisquert, F. F. Santiago, G. G. Belmonte, G. Zoppi, K. Durose, Y. Proskuryakov, I. Oja, A. Belaidi, T. Dittrich, R. T. Zaera, A. Katty, C. L. Clement, V. Barrioz and S. J. C. Irvine, *Nano Lett.*, 2006, **6**, 640-650.
- 41 S. Li, M. S. Toprak, Y. S. Jo, J. Dobson, D. K. Kim and M. Muhammed, *Adv. Mater.*, 2007, **19**, 4347-4352.
- 42 A. H. Yuwono, B. H. Liu, J. M. Xue, J. Wang, H. I. Elim, W. Ji, Y. Li and T. J. White, *J. Mater. Chem.*, 2004, **14**, 2978-2987.
- 43 L. L. Hench and J. K. West, *Chem. Rev.*, 1990, **90**, 33-72.
- 44 P. Zhang, W. C. Li, X. Y. Zhai, C. J. Liu, L. M. Dai and W. G. Liu, *Chem. Commun.*, 2012, **48**, 10431-10433.
- 45 D. Y. Pan, J. C. Zhang, Z. Li, Z. W. Zhang, L. Guo and M. H. Wu, *J. Mater. Chem.*, 2011, **21**, 3565-3567.
- 46 V. N. Mochalin and Y. Gogotsi, *J. Am. Chem. Soc.*, 2009, **131**, 4594-4595.
- 47 Y. Zhang, X. Wang, Y. X. Liu, S. Y. Song and D. Liu, *J. Mater. Chem.*, 2012, **22**, 11971-11977.

